Biochimica et Biophysica Acta, 1102 (1992) 107–114

BBABIO 43650

Low-lying electronic states of carotenoids

Beverly DeCoster [a], Ronald L. Christensen [a], Ronald Gebhard [b], Johan Lugtenburg [b], Roya Farhoosh [c] and Harry A. Frank [c]

[a] *Department of Chemistry, Bowdoin College, Brunswick, ME (USA),* [b] *Gorlaeus Laboratories, University of Leiden, Leiden (The Netherlands) and* [c] *Department of Chemistry, University of Connecticut, Storrs, CT (USA)*

(Received 13 April 1992)

Key words: Carotenoid; Energy transfer; Excited state; Fluorescence; Light harvesting; Photosynthetic bacterium

Four all-*trans* carotenoids, spheroidene, 3,4-dihydrospheroidene, 3,4,5,6-tetrahydrospheroidene, and 3,4,7,8-tetrahydrospheroidene, have been purified using HPLC techniques and analyzed using absorption, fluorescence and fluorescence excitation spectroscopy of room temperature solutions. This series of molecules, for which the extent of π-electron conjugation decreases from 10 to seven carbon-carbon double bonds, exhibits a systematic crossover from $S_2 \rightarrow S_0$ ($1^1B_u \rightarrow 1^1A_g$) to $S_1 \rightarrow S_0$ ($2^1A_g \rightarrow 1^1A_g$) emission with decreasing chain length. Extrapolation of the $S_1 \rightarrow S_0$ transition energies indicates that the 2^1A_g states of longer carotenoids have considerably lower energies than previously thought. The energies of the S_1 states of spheroidenes and other long carotenoids are correlated with the S_1 energies of their chlorophyll partners in antenna complexes of photosynthetic systems. Implications for energy transfer in photosynthetic antenna are discussed.

Introduction

Carotenoids enhance the light-capturing ability of chlorophylls in antenna pigment-protein complexes of photosynthetic organisms by collecting light at wavelengths (~ 400-1500 nm) where chlorophylls are inefficient absorbers [1]. The energy is then transferred from the carotenoids to the chlorophylls, ultimately reaching reaction centers, where it is converted, via electron transfer, into a transmembrane potential [2]. The migration of energy in the antenna prior to trapping by the reaction centers involves the transfer of singlet state energy among the pigments and usually is discussed in terms of the Förster and/or Dexter energy transfer mechanisms [3].

The Förster (or coulombic) mechanism of energy transfer is described by through-space interactions between the donor and acceptor electronic transition dipoles [4]. The magnitudes and relative orientations of the transition dipoles are important in determining the probability with which the energy transfer will occur. In contrast, the Dexter (or exchange) mechanism involves the simultaneous exchange of two electrons between the donor and acceptor pair and requires close proximity between donor and acceptor, which promotes orbital overlap. Which of these mechanisms best describes energy transfer in the antenna complexes in vivo depends on the excited state structures of the molecules, the geometry of the donor/acceptor pair, and competing relaxation pathways of the carotenoids involved in the transfer process. In both cases the rate of energy transfer is proportional to the overlap between the fluorescence spectrum of the donor and the absorption spectrum of the chlorophyll acceptor. The excited state energies of the carotenoids thus play key roles in determining energy transfer efficiencies.

Any discussion of the energies and dynamics of carotenoid excited states must take as its starting point the previous experimental and theoretical work on simple polyenes [5–16] and model carotenoids [17]. Electronic spectroscopy of these molecules has firmly established (for polyenes with four to eight conjugated double bonds) the existence of a 2^1A_g (S_1) state between the ground electronic state (1^1A_g (S_0)) and the lowest one-photon-allowed excited state (1^1B_u (S_2)). In condensed phases, the strong, symmetry-allowed, $S_0 \rightarrow S_2$ absorption typically is accompanied by a 'Stokes-shifted,' symmetry-forbidden, $S_1 \rightarrow S_0$ emission, with fluorescence yields and lifetimes depending on the solvent environment, the length of conjugation, the extent of substitution, and other details of molecular structure. Spectra of intermediate length polyenes

Correspondence to: R.L. Christensen, Department of Chemistry, Bowdoin College, Brunswick, ME 04011, USA.

clearly show a trend toward increasing S_2-S_1 energy separation with increasing conjugation.

Whereas the excited states of shorter polyenes (4–8 conjugated double bonds) are now reasonably well understood, the relationships between the energies and relaxation kinetics of carotenoid excited states and their important roles as energy donors in photosynthesis remain to be elucidated. Longer carotenoids, e.g., β-carotene (11 conjugated double bonds), exhibit weak fluorescences that are not shifted from the origins of their strongly-allowed $1^1A_g \rightarrow 1^1B_u$ absorptions [18–24]. These emissions originate from the S_2 state. The absence of detectable $S_1 \rightarrow S_0$ emissions leaves open to question whether the energies and lifetimes of the 2^1A_g states are compatible with efficient carotenoid-to-chlorophyll energy transfer from this state. A previous investigation of resonance Raman profiles in β-carotene led to the suggestion that its 2^1A_g state lies $\sim 3500\ cm^{-1}$ below the 1^1B_u state, well above the S_1 (Q_y) states of most chlorophylls [25,26]. The apparent energetic suitability of carotenoid S_1 states for energy transfer has been widely cited in discussions of the antenna function of these molecules in photosynthesis [27–29]. However, more recent resonance Raman measurements have shown that this technique cannot detect the weak $1^1A_g \rightarrow 2^1A_g$ transition on top of the low-energy tail of the strong $1^1A_g \rightarrow 1^1B_u$ absorption [30]. Furthermore, the extensive data now available for intermediate length polyenes [5–16], for which the 2^1A_g states can be accurately located from the origins of the $S_1 \leftrightarrow S_0$ emission and excitation spectra, point to S_1 energies in long polyenes that are considerably lower than previously assumed. It seems fair to say that for molecules such as β-carotene and spheroidene, the energies, and thus the roles of the 2^1A_g states in energy transfer, are rather uncertain.

The present work focuses on the electronic energies and decay characteristics of the 2^1A_g and 1^1B_u states of four all-*trans* carotenoids: spheroidene, 3,4-dihydrospheroidene ('methoxyneurosporene'), 3,4,5,6-tetrahydrospheroidene and 3,4,7,8-tetrahydrospheroidene (Fig. 1). Spheroidene and 3,4-dihydrospheroidene have ten and nine conjugated π-electron double bonds and occur naturally in cells of purple, non-sulfur, photo synthetic bacteria. 3,4,5,6-Tetrahydrospheroidene and 3,4,7,8-tetrahydrospheroidene are synthetic analogs having eight and seven conjugated π-electron double bonds, respectively. An important feature of this work has been the development of HPLC techniques which allow the study of isomerically pure samples. The all-*trans* isomers of these four molecules, which are structurally identical except for their systematic variation in the extent of π-electron conjugation, provide important guideposts toward an understanding of how carotenoids collect and transfer energy in photosynthetic systems.

Materials and Methods

Cells of the *Rhodobacter sphaeroides* bacteria were grown as previously described [31]. Spheroidene was extracted from whole cells of *Rb. sphaeroides* wild type strain 2.4.1 and 3,4-dihydrospheroidene (methoxyneurosporene) was extracted from cells of *Rb. capsulatus* MT1131. Spheroidene was isolated in the following manner: to the pelleted whole cells of *Rb. sphaeroides* wild type strain 2.4.1 an equal volume of acetone was added and the mixture centrifuged at $18000 \times g$ for 5 min. The supernatant was then poured off and additional extractions were performed until the supernatant was yellow and the pellet was tan. After reducing its volume by rotory evaporation, the acetone layer was partitioned with an equal volume of pentane and separated. The pentane layer was washed with water and then extracted several times with methanol/water (95/5%) until the methanol extract was no longer green. The pentane layer was then evaporated to dryness. The solid carotenoid residue was redissolved in petroleum ether (b.p. 40–60°C) and applied to an alumina (Sigma A-9003) column. Spheroidene was obtained by eluting with a $\sim 2\%$ solution of ethyl acetate in petroleum ether. The 3,4-dihydrospheroidene was obtained by a similar extraction procedure and purified by thin layer chromatography on silica gel, using 1:1 chloroform/toluene as the eluting solvent. Samples were stored as dilute solutions in petroleum ether. The synthesis and purification of 3,4,5,6-tetrahydrospheroidene and 3,4,7,8-tetrahydrospheroidene have been described [32,33].

Petroleum ether solutions of each carotenoid were evaporated in a stream of nitrogen and the residue redissolved in methanol. These samples were injected into a Hewlett Packard HP1090 Liquid Chromatograph equipped with a diode-array detector which provided 2 nm optical resolution. The separation was carried out

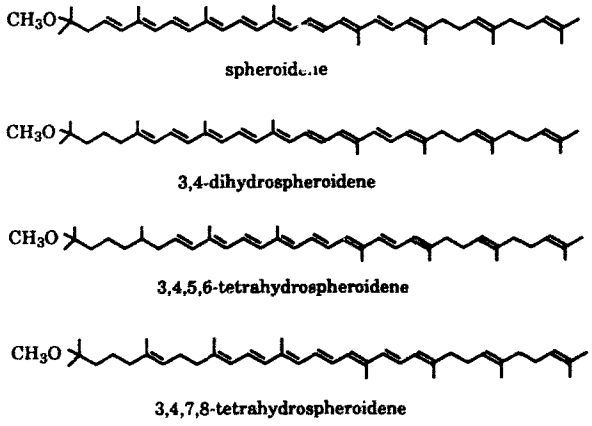

Fig. 1. Molecules studied.

using a C_{18} reversed-phase column (200 × 4.6 mm) and guard column (both containing Lichrosorb RP-18, 5 μm particles). Samples were eluted at a flow rate of 2.0 ml/min. with a mobile phase programmed as follows: 0–4 min, isocratic, methanol/*n*-hexane (95/5 v/v), 4–6 min, linear gradient to methanol/water (95/5 v/v), 6–10 min, linear gradient to methanol/water (98/2 v/v). Chromatograms initially were monitored at wavelengths where the four spheroidenes gave maximum absorbance. The diode-array detector also allowed the recording of complete spectra (190–600 nm) of individual components which was helpful in assigning components to *cis* and *trans* spheroidene isomers. Individual peaks were collected in quartz cuvettes and fluorescence and fluorescence excitation spectra taken immediately. Reinjection of solutions following fluorescence measurements allowed monitoring of samples for photochemical and thermal degradation.

Fluorescence and fluorescence excitation spectra were obtained on a SPEX Model 212 spectrofluorimeter. Interferences from Raman scattering from the solvent were corrected for by subtraction of a solvent blank taken under identical conditions. Fluorescence spectra were also corrected for the wavelength dependencies of optical components using correction factors obtained by recording the spectrum of a standard lamp. Fluorescence excitation spectra were obtained in ratio mode using a Rhodamine B quantum counter and generally were in good agreement with absorption spectra obtained on a Shimadzu UV240 spectrophotometer. In some cases spectra were smoothed (using a 25 point Savitsky-Golay algorithm [34,35]) to enhance signal/noise. Fluorescence spectra also were subjected to second derivative/smoothing techniques to locate spectral features which could be identified with the $S_1 \rightarrow S_0$ electronic origins.

Results

A typical HPLC separation of the spheroidene sample is given in Fig. 2. The ultraviolet-visible spectra of the four peaks with retention times greater than 10 min are rather similar and, as is the case for other long polyenes, are dominated by the distinctive, strongly-allowed, $1^1A_g \rightarrow 1^1B_u$ transition in the 400–500 nm region (Fig. 3). The longest-wavelength vibrational features of this transition (the electronic origins) range from 475 to 481 nm for the four components. The most striking differences between the spectra of the components are the relative intensities in the so-called '*cis*-band region,' ~ 310–360 nm. For example, the second component has very little intensity in this region, compared with the other three components. This observation, plus the dominance of the second component in all of our samples, leads to the assignment of this peak as all-*trans* spheroidene. The other components most likely are various *cis* spheroidene isomers with the strength of the '*cis*-band' indicating the extent of deviation of the spheroidene from the idealized C_{2h} symmetry of the all-*trans* isomer. Spectra with the strongest *cis*-bands presumably can be identified with molecules that are isomerized about central double bonds [36].

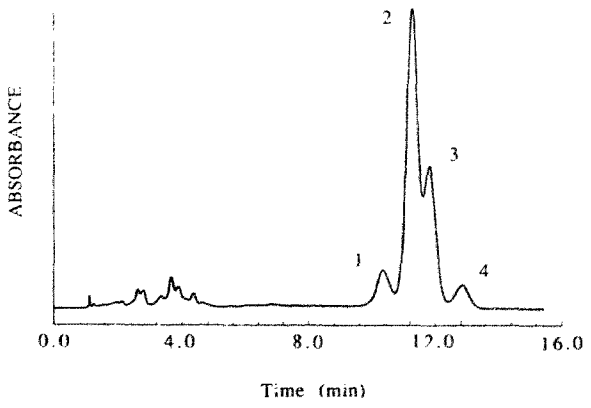

Fig. 2. HPLC of spheroidene sample. The mobile and stationary phases are described in the experimental section. The chromatogram was detected at 450 nm (peak 2 has a maximum absorbance of 0.18).

In addition to separating the various spheroidene isomers, the HPLC procedures resolve many other species with shorter elution times. These fractions absorb at shorter wavelengths (< 400 nm) and most likely are less conjugated polyenes, including spheroidene degradation products that were not eliminated in previous purification steps. Chromatograms monitored at shorter wavelengths show that the concentrations of these impurities are not insignificant. Furthermore, shorter polyenes tend to have higher fluorescence yields [5,7,14] and thus can interfere with fluorescence and fluorescence excitation spectra, particularly in the short wavelength regions around the spheroidene '*cis* peaks.'

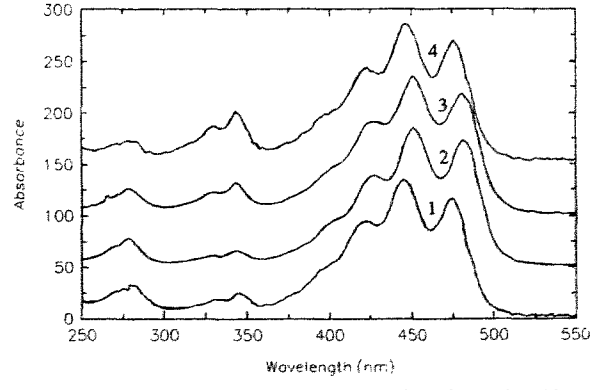

Fig. 3. Ultraviolet/visible absorption spectra of the four spheroidene isomers indicated in Fig. 2. Spectra were recorded by a diode-array detector at times corresponding to the maxima in the chromatogram. Spectra have been scaled to give the same maximum absorption.

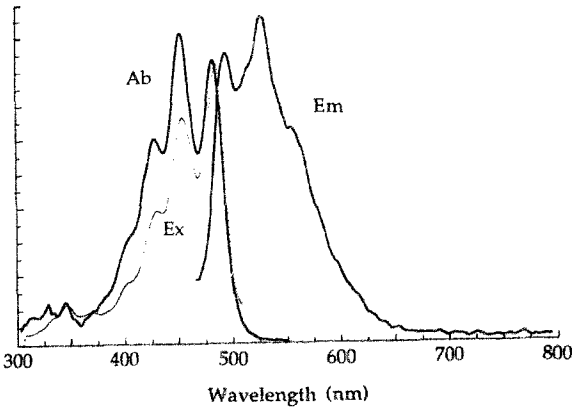

Fig. 4. Absorption (Ab, solid line), fluorescence (Em), and fluorescence excitation (Ex, dotted line) spectra of all-*trans*-spheroidene in methanol. The fluorescence spectrum was obtained by exciting at 450 nm. The fluorescence excitation spectrum was obtained by monitoring the emission at 560 nm.

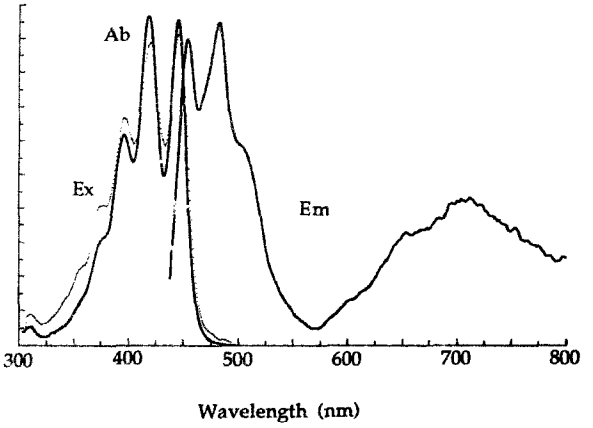

Fig. 6. Absorption (Ab, solid line), fluorescence (Em), and fluorescence excitation (Ex, dotted line) spectra of all-*trans*-3,4,5,6-tetrahydrospheroidene in methanol. The fluorescence spectrum was obtained by exciting at 417 nm. The fluorescence excitation spectrum was obtained by monitoring the emission at 710 nm.

Chromatography of the other spheroidenes gave similar results, i.e., the separation of geometric isomers, as well as less conjugated, more fluorescent, impurities. Comparison of chromatograms taken before and after fluorescence measurements allowed monitoring of samples for thermal and photochemical (e.g., *cis-trans* isomerization) degradation. The spectra presented below thus can be identified with pure, all-*trans* isomers of the various spheroidene derivatives and yield unambiguous assignments of the emission characteristics of these molecules. Such stringent criteria for sample purities have not been met in previous efforts to understand the details of carotenoid fluorescence.

The room temperature fluorescence, fluorescence excitation, and absorption spectra of the four, all-*trans* spheroidenes are presented in Figs. 4–7. For spheroidene (Fig. 4), the fluorescence spectrum is a mirror-image of the $S_0 \rightarrow S_2$ absorption. The overlap between the origins of emission and absorption leads to a $S_2 \rightarrow S_0$ assignment for the fluorescence. There is no evidence for a longer wavelength $S_1 \rightarrow S_0$ emission in this molecule. The absorption and fluorescence excitation spectra are in good agreement, as expected for these well-purified samples. There are some traces of contaminants that compete with spheroidene fluores-

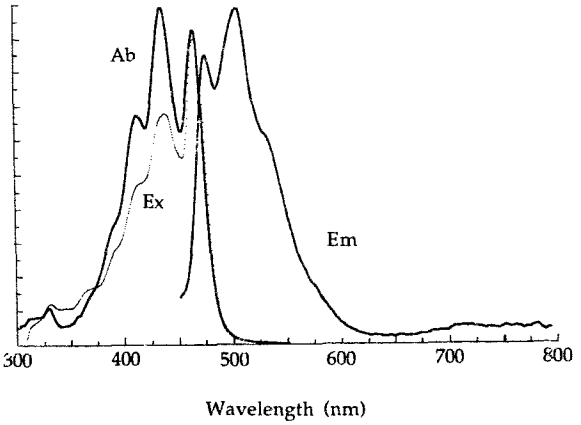

Fig. 5. Absorption (Ab, solid line), fluorescence (Em), and fluorescence excitation (Ex, dotted line) spectra of all-*trans*-3,4-dihydrospheroidene in methanol. The fluorescence spectrum was obtained by exciting at 437 nm. The fluorescence excitation spectrum was obtained by monitoring the emission at 530 nm. Excitation spectra obtained monitoring the weak emission between 700 and 800 nm were similar to the excitation spectrum presented here.

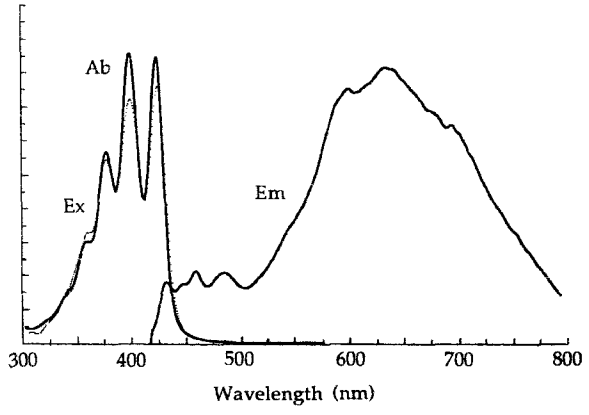

Fig. 7. Absorption (Ab, solid line), fluorescence (Em), and fluorescence excitation (Ex, dotted line) spectra of all-*trans*-3,4,7,8-dihydrospheroidene in methanol. The fluorescence spectrum was obtained by exciting at 400 nm. The fluorescence excitation spectrum was obtained by monitoring the emission at 700 nm.

cence when samples are excited below 400 nm. Above 400 nm, however, the fluorescence spectrum is independent of the wavelength of excitation, as expected for emission from a single, all-*trans* spheroidene species.

The spectra of 3,4-dihydrospheroidene ('methoxyneurosporene', Fig. 5) are similar to those of spheroidene. However, there are indications in the 700–800 nm region of a weak, longer wavelength emission, indicating $S_1 \rightarrow S_0$ fluorescence ($2^1A_g \rightarrow 1^1A_g$) in this molecule. It is important to note that 3,4-dihydrospheroidene (nine conjugated double bonds) is the longest carotenoid for which the low energy 2^1A_g state has been observed. The presence of $S_1 \rightarrow S_0$ emission in methoxyneurosporene is supported by comparing its fluorescence spectrum with those of its the less-conjugated homologs, 3,4,5,6-tetrahydrospheroidene (Fig. 6) and 3,4,7,8-tetrahydrospheroidene (Fig. 7). Excitation of the latter compound gives almost exclusively $S_1 \rightarrow S_0$ fluorescence as observed for other methyl-substituted heptaenes. It also should be noted that the emissions ($S_2 \rightarrow S_0$ and $S_1 \rightarrow S_0$) of 3,4,5,6-tetrahydrospheroidene are very similar to the dual fluorescences previously observed for β-11′-carotene, another carotenoid with eight conjugated double bonds (S. Cosgrove, D.S. Smith, and R.L. Christensen, unpublished data).

Discussion

The four spheroidenes show a clear pattern in their fluorescences, i.e., a crossover from the S_1 emissions observed in shorter, model polyenes to the S_2 emissions in more extensively conjugated systems. A similar pattern was observed in our previous study of a series of carotenols with seven to 11 conjugated double bonds [17]. The spheroidene series shows a systematic dependence of the S_1 and S_2 electronic energies on the length of conjugation (Table I and Fig. 8). In determining the energies of the spheroidene $S_1 \rightarrow S_0$ electronic origins, we have compared our fluorescence spectra (and their second derivatives) with spectra of analogous model polyenes [17]. The $S_1 \rightarrow S_0$ (0-0)'s of the simpler systems are well-resolved, even in room temperature solutions, and the relative intensities of these and other vibronic bands guide our assignments of (0-0) bands in the spheroidenes. In addition, the well-understood α,ω-dimethylpolyenes series provides an important benchmark for the dependence of polyene S_2 and S_1 energies on the length of conjugation. The almost identical trends noted in the two series further validate our assignments of the spheroidene electronic origins. Extrapolation of the 2^1A_g energies to molecules such as spheroidene, spirilloxanthin (13 conjugated double bonds), and β-carotene (11 conjugated bonds), and comparison of the S_1 energies of these polyenes with the S_1 energies of various chlorophylls, forms the primary focus for this discussion.

The 1^1B_u (S_2) and the 2^1A_g (S_1) states of spheroidenes are systematically lower than the corresponding S_2 and S_1 states of simpler, less substituted polyenes with the same extent of conjugation (Fig. 8). The lowering of polyene 1^1B_u energies in the more extensively substituted carotenoids has been noted previously [17]. The effect of alkyl substituents on 2^1A_g energies is not as well understood, though a comparison of dimethyl and unsubstituted tetraenes, pentaenes, hexaenes, and heptaenes (molecules for which the $1^1A_g \rightarrow 2^1A_g$ electronic origins are easily located from well-resolved, low-temperature fluorescence spectra) suggests that the 2^1A_g state energies are not as sensitive as the 1^1B_u states to the effects of substitution

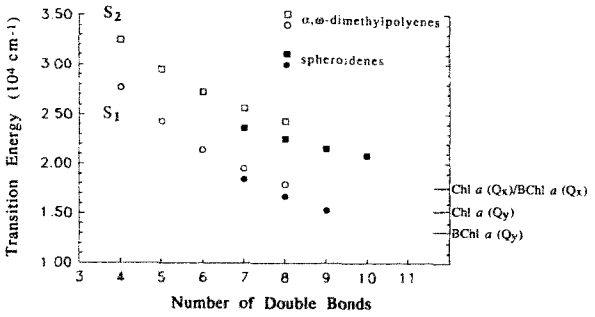

Fig. 8. $S_0 \rightarrow S_1$ ($1^1A_g \rightarrow 2^1A_g$) and $S_0 \rightarrow S_2$ ($1^1A_g \rightarrow 1^1B_u$) transition energies for α,ω-dimethylpolyenes and spheroidenes as a function of conjugated length. Energies of the S_1 states are the electronic origins (0-0 bands) observed for $S_1 \rightarrow S_0$ fluorescence in room temperature methanol. Energies of the S_2 states are the electronic origins (0-0 bands) observed for $S_0 \rightarrow S_2$ absorption in room temperature methanol. Dimethylpolyene data are from Morey and Christensen (unpublished) and Ref. 16. Chlorophyll *a* (Q_x = 575 nm, Q_y = 660 nm) and bacteriochlorophyll *a* (Q_x = 573 nm, Q_y = 769 nm) transition energies in diethyl ether at room temperature are taken from Ref. 45.

TABLE I

$S_1 \rightarrow S_0$ and $S_0 \rightarrow S_2$ transition energies of α,ω-dimethylpolyenes and spheroidenes as a function of conjugated length

Transition energies refer to room temperature methanol solutions. Dimethylpolyene data are from Morey and Christensen (unpublished) and Ref. 16.

Number of double bonds	Transition energy (10^4 cm^{-1})			
	α,ω-dimethylpolyenes		spheroidenes	
	$S_1 \rightarrow S_0$	$S_0 \rightarrow S_2$	$S_1 \rightarrow S_0$	$S_0 \rightarrow S_2$
4	2.770	3.255		
5	2.425	2.954		
6	2.141	2.722		
7	1.949	2.558	1.84	2.36
8	1.794	2.434	1.67	2.25
9			1.53	2.15
10				2.08

(T. Morey and R.L. Christensen, unpublished data). It also is worth noting the case of isotachysterol, a fully substituted all-*trans* hexatriene [37]. In this molecule the 1^1B_u state is shifted dramatically to the red, but the 2^1A_g state is virtually unshifted relative to the corresponding states observed in less substituted, model trienes. These effects carry over to the spheroidenes and result in smaller S_2-S_1 energy differences than those of less substituted polyenes with the same length of conjugation.

The cross-over to $S_2 \rightarrow S_0$ emissions in the longer polyenes has been attributed to the increase in the S_2-S_1 energy difference with increasing polyene length [14,17]. This results in a decrease in the rate of $S_2 \rightarrow S_1$ internal conversion following the well-known 'energy gap law.' [38–40] For large energy gaps ($> 5000\ cm^{-1}$), internal conversion rates apparently become sufficiently small to allow $S_2 \rightarrow S_0$ fluorescence to compete with radiationless decay processes. The energy gap model has been applied to several aromatic compounds that violate Kasha's Rule (Kasha's Rule states that large molecules in condensed phase fluoresce from their lowest excited singlet states) and appears to give a quantitative account of $S_2 \rightarrow S_1$ internal conversion in these systems. For linear polyenes, on the other hand, the rather abrupt changeover from $S_1 \rightarrow S_0$ to $S_2 \rightarrow S_0$ emissions with increasing conjugation is not easily reconciled with modest increases in the S_2-S_1 energy gap [17]. This suggests that at least some of the parameters contained in the energy gap law derivation for aromatic molecules (changes in molecular geometry, vibronic coupling parameters, nature of the 'acceptor modes,' etc.) do not apply to polyenes. These differences are further highlighted by comparing the excited state dynamics of β-carotene and perdeutero-β-carotene [41–43]. The almost identical S_1 lifetimes of these molecules suggest that, in contrast to aromatics, C–H vibrations do not play dominant roles as acceptor modes in polyene radiationless decay processes. However, a large S_2–S_1 energy difference appears to be the common element for detectable emission from S_2 in both aromatic and polyene systems.

The energies of the 2^1A_g states of spheroidene, β-carotene, spirilloxanthin and other naturally occurring polyenes are of fundamental importance in understanding how these carotenoids function in photosynthetic systems. For example, the mechanism of energy transfer from spheroidene to bacteriochlorophyll *a* in the B800-850 light-harvesting complex of *Rhodobacter sphaeroides* wild type strain 2.4.1 and the details of how energy moves from β-carotene to chlorophyll *a* in green plants are, as yet, unclear. The present determination of the low energy of 2^1A_g states in longer polyenes leads to the possibility that in some cases carotenoid S_1 states lie below those of their energy-accepting, chlorophyll partners.

The absence of detectable $S_1 \rightarrow S_0$ fluorescence from long polyenes, such as spheroidene and β-carotene, thwarts the direct detection of the 2^1A_g states in these systems, at least by conventional, one-photon, optical techniques. One, thus, must rely on the extrapolation of the 2^1A_g energies observed for shorter dimethylpolyenes and spheroidene derivatives (Fig. 8). This indicates that the 2^1A_g state of spheroidene (10 double bonds) most likely is higher in energy than the S_1 (Q_y) state of bacteriochlorophyll. Carotenoid-to-bacteriochlorophyll energy transfer in *Rhodobacter sphaeroides* most likely occurs via the spheroidene 2^1A_g state. On the other hand, the data presented in Fig. 8 suggests that the S_1 state of β-carotene (11 double bonds) lies below the S_1 state (Q_y) of its chlorophyll acceptor.

Initial investigations of the resonance Raman profiles of β-carotene indicated that its 2^1A_g state lies at $\sim 17230\ cm^{-1}$, $3500\ cm^{-1}$ below the origin of the 1^1B_u state [25,26]. This places the 2^1A_g state well above the $\sim 15150\ cm^{-1}$ (660 nm) S_1 state of chlorophyll *a*, an energy scheme that has been widely cited in discussions of energy transfer in green plant photosynthesis [27–29]. However, the early resonance Raman results cannot be repeated [30] and a $17000\ cm^{-1}$ 2^1A_g state in β-carotene clearly is incompatible with the data summarized in Fig. 8 which indicate a β-carotene 2^1A_g state in the $13000–14000\ cm^{-1}$ range. Spirilloxanthin should have an even lower energy 2^1A_g state. Low 2^1A_g energies (and correspondingly large S_2-S_1 energy differences) also are consistent with the absence of S_1 emission in these systems.

The dominance of $S_2 \rightarrow S_0$ emissions and low S_1 energies in long carotenoids have obvious implications for mechanisms of light harvesting in photosynthetic antenna complexes. As first pointed out by Snyder et al. in 1985 [14], the reduction in $S_2 \rightarrow S_1$, internal conversion rates opens up the possibility that for long polyenes fluorescence and energy transfer both may originate from the S_2 state. For β-carotene this may well become a necessity, given that its S_1 state most likely lies well below the lowest excited singlet state (Q_y) of chlorophyll *a*. The 2^1A_g states of more extensively conjugated molecules, such as spirilloxanthin, also might be too low to play significant roles as energy donors in bacterial photosynthetic, light-harvesting proteins. This could explain the fact that the energy transfer efficiencies observed for B800-850 complexes isolated from spirilloxanthin-containing species of photosynthetic bacteria are reduced to 20–50% from the ~ 100% value observed for spheroidene-containing complexes [1]. In contrast to β-carotene/chlorophyll *a*, however, the considerably lower energy of the bacteriochlorophyll S_1 (Q_y) acceptor may still allow energy transfer from the 2^1A_g state of spirilloxanthin. The low energy transfer effeciency then might be explained by the poor overlap between donor fluorescence and ac-

ceptor absorption of almost isoenergetic electronic states (see below). This would allow polyene internal conversion to compete with energy transfer.

Both the Dexter and the Förster mechanisms for energy transfer depend on the overlap between the fluorescence spectrum of the donor and the absorption spectrum of the acceptor [4]. For polyenes, geometry changes associated with the $S_1 \rightarrow S_0$ transition typically result in broad fluorescence spectra (see Figs. 5–7) with relatively weak intensity at wavelengths corresponding to transitions between the zero-point levels of the S_1 and S_0 states (0-0 band). This is in contrast with the absorption and emission spectra of chlorophylls, for which a large fraction of the Q_y transition strength is concentrated in the (0-0) and (0-1) bands. As a consequence, the overlap between carotenoid $S_1 \rightarrow S_0$ emission and chlorophyll $S_0 \rightarrow S_1$ absorption may be small, even in cases where the S_1 energy of the donor is equal to or slightly greater than the S_1 energy of the acceptor. S_1(carotenoid) to S_1(chlorophyll) energy transfer will be enhanced when the acceptor (0-0) band is 1000–3000 cm^{-1} below the (0-0) band of the carotenoid $S_1 \rightarrow S_0$ fluorescence. Spheroidene-containing B800-850 complexes of *Rhodobacter sphaeroides* clearly satisfy this criterion [44]. The weak, forbidden nature of the polyene $S_1 \rightarrow S_0$ transition further requires short-range electron exchange (Dexter transfer) rather than coulombic interactions for transfer involving a carotenoid 2^1A_g state. The high efficiency of energy transfer indicates transfer rates that are considerably faster than the $\sim 10^{11}$ s^{-1} $S_1 \rightarrow S_0$ internal conversion rates for typical, isolated carotenoids [41–43].

For energy transfer between β-carotene and chlorophyll *a*, the 15000 cm^{-1} S_1 state (Q_y) of chlorophyll must lie well above the S_1 state of the polyene (see Fig. 8). This implicates the carotene S_2 state as the donor state. Although the rate of $S_2 \rightarrow S_1$ internal conversion is reduced by the relatively large S_2-S_1 energy difference, the S_2 state is still relatively short-lived. Fluorescence yields of β-carotene [17,22] and recent time-resolved measurements on spheroidene in vitro [46] give 200–400 fs lifetimes for the S_2 state. How can S_2 energy transfer compete with S_2 internal conversion? Spectral overlap between the $S_2 \rightarrow S_0$ emission of the carotenoid (Figs. 4 and 5) and higher energy, Q_x transitions of the carotenoid would be large. The carotenoid and chlorophyll are most likely in intimate contact in the antenna complexes. Strong coulombic interactions (Förster coupling) between close, well-oriented transition dipoles of the chlorophyll Q_x absorption and the symmetry-allowed $S_2 \rightarrow S_0$ emission could lead to rapid energy transfer. Energy transfer in photosynthetic systems typically is discussed as a choice between the electron exchange and coulombic mechanisms. However, the interactions between strongly coupled electronic transitions at short distances also may include terms due to weak excitonic interactions [39,47]. (Förster transfer is a special case in the 'weak-coupling' limit.) Excitonic interactions (resonance couplings between carotenoid and chlorophyll vibronic states) would further accelerate energy transfer from S_2.

Summary

Absorption and fluorescence spectroscopy of short, model polyenes [5–16], carotenols [17], and spheroidenes have provided a detailed understanding of how the electronic energies of polyene S_2 (1^1B_u) and S_1 (2^1A_g) states depend on conjugated length (Fig. 8). Extrapolation of these results to molecules, such as spirilloxanthin and β-carotene, indicates that the S_1 states of these longer polyenes have considerably lower energies than previously thought. Longer carotenoids also exhibit S_2 fluorescence. This is consistent with their low S_1 energies, relatively large S_2-S_1 energy gaps, and associated reductions in $S_2 \rightarrow S_1$ internal conversion rates.

For spheroidene-containing, B800-850 complexes of *Rhodobacter sphaeroides*, spheroidene S_1 states have sufficient energy and lifetimes to funnel excitation into the S_1 states of chlorophyll acceptors. For β-carotene/chlorophyll *a* complexes in green plants, the lower polyene S_1 (2^1A_g) energy makes it unlikely that this state plays an important role in energy transfer. The reduction in $S_2 \rightarrow S_1$ internal conversion rates and the close proximity of carotenoids and chlorophylls may allow transfer via the carotenoid S_2 state. This would require strong coupling between the $S_2 \rightarrow S_0$ transitions of the polyene and $S_0 \rightarrow S_n$ absorptions (probably the Q_x bands) of the chlorophylls.

Regardless of the mechanism of singlet energy transfer, it is remarkable that carotenoids function as efficient energy donors in photosynthesis in a wide variety of carotenoid/chlorophyll combinations. Both the S_2 (1^1B_u) and the S_1 (2^1A_g) states of long polyenes have a great propensity to lose electronic energy through fast, non-radiative decay (internal conversion) and might appear to be ill-suited for their important roles as antenna pigments. These deficiencies apparently are overcome by arranging donor/acceptor complexes in geometries which allow energy transfer to compete with (and in many cases overwhelm) rapid thermal relaxation to carotenoid ground states.

Acknowledgements

RLC acknowledges the donors of the Petroleum Research Fund, administered by the American Chemical Society, and a DuPont Fund grant to Bowdoin College for support of this research. This work also has

been sponsored by the Netherlands Foundation for Chemical Research (SON), with financial aid from the Netherlands Organization for Scientific Research (ZWO). We thank Joost van Dijk for assistance with the synthesis of the modified spheroidenes. HAF acknowledges grants from the National Institutes of Health (GM-30353), the Competitive Research Grants Office of the US Department of Agriculture (88-37130-3938), the NATO Scientific Affairs Division (880107) and the University of Connecticut Research Foundation.

References

1 Cogdell, R.J. and Frank, H.A. (1987) Biochim. Biophys. Acta 895, 63–79.
2 Feher, G. and Okamura, M.Y. (1978) in The Photosynthetic Bacteria (Clayton, R.K. and Sistrom, W.R., eds.), pp. 349–386, Plenum Press, New York.
3 Van Grondelle, R. (1985) Biochim. Biophys. Acta 811, 147–195.
4 Turro, N.J. (1978) Modern Molecular Photochemistry, pp. 296–358, Benjamin/Cummings, Menlo Park.
5 Gavin, Jr., R.M., Weisman, C., McVey, J.K. and Rice, S.A. (1978) J. Chem. Phys. 68, 522–529.
6 Granville, M.F., Holtom, G.R., Kohler, B.E., Christensen, R.L. and D'Amico, K.L. (1979) J. Chem. Phys. 70, 593.
7 D'Amico, K.L., Manos, C. and Christensen, R.L. (1980) J. Am. Chem. Soc. 102, 1777.
8 Heimbrook, L.A., Kenny, J.E., Kohler, B.E. and Scott, G.W. (1981) J. Chem. Phys. 75, 4338–4342.
9 Hudson, B.S., Kohler, B.E. and Schulten, K. (1982) in Excited States (Lim, E.C., ed.), Vol. 6, pp 1–95, Academic Press, New York,
10 Heimbook, L.A., Kohler, B.E. and Spiglanin, T.A. (1983) Proc. Natl. Acad. Sci. USA 80, 4580–4584.
11 Leopold, D.G., Vaida, V. and Granville, M.F. (1984) J. Chem. Phys. 81, 4210–4217.
12 Leopold, D.G., Pendley, R.D. and Roebber, J.L., Hemley, R.J. and Vaida, V. (1984) J. Chem. Phys. 81, 4218–4229.
13 Heimbrook, L.A., Kohler, B.E. and Levy, I.J. (1984) J. Chem. Phys. 81, 1592–1597.
14 Snyder R., Arvidson, E., Foote, C., Harrigan, L., Christensen, R.L. (1985) J. Am. Chem. Soc. 107, 4117–4122.
15 Simpson, J.H., McLaughlin, L., Smith, D.S. and Christensen, R.L. (1987) J. Chem. Phys. 87, 3360–3365.
16 Kohler, B., Spangler, C. and Westerfield, C. (1988) J. Chem. Phys. 89, 5422–5428.
17 Cosgrove, S.A., Guite, M.A., Burnell, T.B. and Christensen, R.L. (1990) J. Phys. Chem. 94, 8118–8124.
18 Cherry, R.J., Chapman, D. and Langemaar, J. (1968) Trans. Far. Soc. 64, 2304.
19 Van Riel, M., Kleinen-Hammans, J., Van de Ven, M., Verwer, W. and Levine, Y. (1983) Biochem. Biophys. Res. Commun. 113, 102–107.
20 Haley, L.V. and Koningstein, J.A. (1983) J. Phys. Chem. 87, 621.
21 Watanabe, J., Kinoshita, S. and Kushida, T. (1986) Chem. Phys. Lett. 126, 197–200.
22 Gillbro, T. and Cogdell, R.J. (1989) Chem. Phys. Lett. 158, 312–316.
23 Bondarev, S.L., Dvornikov, S.S. and Bachilo, S.M. (1988) Opt. Spectrosc. (USSR) 64(2), 268–270.
24 Bondarov, S.L., Bachilo, S.M., Dvornikov, S.S. and Tikhomorov, S.A. (1989) J. Photochem. Photobiol, A: Chemistry 46, 315–322.
25 Thrash, R.J., Fang, H. and Leroi, G.E. (1977) J. Chem. Phys. 67, 5930–5933.
26 Thrash, R.J., Fang, H. and Leroi, G.E. (1979) Photochem. Photobiol. 29, 1049–1050.
27 Sauer, K. (1978) Acc. Chem. Res. 11, 257–264.
28 Cogdell, R.J., Hipkins, M.F., MacDonald, W. and Truscott, T.G. (1981) Biochim. Biophys. Acta 634, 191–202.
29 Siefermans-Harms, D. (1985) Biochim. Biophys. Acta 811, 325.
30 Watanabe, J., Kinoshita, S. and Kushida, T. (1987) J. Chem. Phys. 87, 4471–4477.
31 Frank, H.A., Machnicki, J. and Toppo, P. (1984) Photochem. Photobiol. 39, 429–432.
32 Gebhard, R. (1991) Synthesis and Application of Isotopically and Chemically Modified Spheroidenes, Ph.D. Thesis, University of Leiden.
33 Gebhard, R., Van der Hoef, K., Violette, C.A., De Groot, H.J.M., Frank, H.A. and Lugtenburg, J. (1991) Pure and Appl. Chem. 63, 115–122.
34 Savitsky, A. and Golay, M.J.E. (1964) Anal. Chem. 36, 1727.
35 Steiner, J., Termonia, Y. and Deltour, J. (1972) Anal. Chem. 44, 1906.
36 Zechmeister, L. (1962) *Cis-trans* Isomeric Carotenoids, Vitamins A, and Arylpolyenes, Academic Press, New York.
37 Pierce, B.M., Bennett, J.A. and Birge, R.R. (1982) J. Chem. Phys. 77, 6343–6344.
38 Robinson, G.W. and Frosch, R.P. (1962) J. Chem. Phys. 37, 1962.
39 Robinson, G.W. and Frosch, R.P. (1963) J. Chem. Phys. 38, 1187.
40 Englman, R. and Jortner, J. (1970) Mol. Phys. 18, 145.
41 Wasielewski, M.R. and Kispert, L.D. (1986) Chem. Phys. Lett. 128, 238–243.
42 Hashimoto, H. and Koyama, Y. (1989) Chem. Phys. Lett. 154, 321–325.
43 Wasielewski, M.R., Johnson, D.G., Bradford, E.G. and Kispert, L.D. (1989) J. Chem. Phys. 91, 6691–6697.
44 Frank, H.A., Farhoosh, R., Aldema, M.L., DeCoster, B., Christensen, R.L., Gebhard, R. and Lugtenburg, J. Photochem. Photobiol. (in press).
45 Sauer, K. (1975) in Bioenergetics of Photosynthesis (Govindjee, ed.), pp. 115–181, Academic Press, New York.
46 Shreve, A.P., Trautman, J.K., Frank, H.A., Owens, T.G. and Albrecht, A.C. (1991) Biochim. Biophys. Acta 1058, 280–288.
47 Simpson, W.T. and Peterson, D.L. (1957) J. Chem. Phys. 26, 588–593.